Heterogeneous Collaborative Pose Stabilization of a Bar Via Aerial Manipulation and Tethering

P. Roque and P. O. Pereira and Dimos V. Dimarogonas

Abstract

We consider a system composed by a rod-like object, grasped by one manipulator-endowed UAV at one contact point, and tethered to another UAV at a separate contact point. The system combines the mechanical simplicity of the tethering system with the flexibility of the manipulator, with the objective of stabilizing the pose of the rod-like object around a desired pose. We consider two cases, one where the manipulator is free of actuation, and another where the manipulator is locked. We endow each UAV with PID controllers, and by means of a linearization procedure, determine bounds on the PID gains that guarantee the former stabilization objective is exponentially stable. We also establish a comparison between the system and that of a container-crane system, and observe that the rod-like object behaves similarly to a container, along the longitudinal and vertical directions.

I. Introduction

Unmanned Aerial Vehicles (UAVs) have been successfully used to map and surveil large surface areas, inspect remote infrastructures, and, more recently, to transport and deliver goods. Transportation with multiple UAVs is necessary when the cargo exceeds the individual UAVs' payload capacity, and it provides robustness against failures of one or more of the cooperating UAVs.

Two mains approaches for aerial cooperative transportation have been considered in literature, namely tethered transportation [1]–[7] or transportation by means of manipulators/robotics arms [8]–[12]. On the one hand, tethered systems are easier to couple on a vehicle, as, in general, they do not require any power supply or additional equipment. On the other hand, manipulators allow for more precision placement of the object being manipulated, as there is no need to compensate for the sway caused by the load, but only for the reaction torques from manipulating the object.

Regarding tethering systems, vision has been used in both slung-load transportation and cooperative tethered transportation to estimate the cargo's pose [1], [13], and to track and align the vehicles with fiducial markers placed on the cargo [2]. Force sensors have also been used for the purposes of control in tethered transportation. In [9], a method is proposed that estimates the slung-load swing-angle, recurring to the UAV's IMU and to a load cell, and uses it in the feeback loop to avoid swing excitation In [4], a master-slave approach is implemented with the UAV-slave complying with the UAV-master motion by means of an admittance controller. Finally, how to position a group of UAVs such that a tethered cargo acquires a desired pose has been studied in [14].

On what respects transportation recurring to manipulators, single-UAV control, estimation and stability have been studied in [15], [16]. Methods for visual-servoing object grasping were developed in [17]–[19]. Mechanical grasping resorting to delta manipulators was proposed in [20], and magnetic handling by means of an electro-permanent magnet in [21], where the latter is electrically activated/de-activated and it has no steady-state power consumption. Planning of collision free trajectories between the cargo and the vehicles has been studied in [6], [8], [22]. Finally, tele-operation has been used to control of a group of UAVs transporting a cargo [11], [12].

Heterogeneous systems can combine the best characteristics of each type of system. [23] provides a first approach to an heterogenous system, resorting to a ground platform aided by an aerial vehicle to transport and manipulate objects.

This work focuses on heterogenous aerial systems, combining two different UAVs with different manipulation capabilities – one vehicle with an aerial manipulator and another with a cable. For the modeling of the system we follow a similar formalism as that in [24]. The control objective is to stabilize the bar's pose, as pictured in Fig. 1, around a desired pose. We perform an analysis similar to that in [16], [25], [26], where we linearize the system, and derive conditions on the gains that guarantee exponential stability regarding the stabilization of the bar's pose. We also verify that the bar behaves similarly to non-point-mass container (i.e., a container with inertia) in a container-crane system [24], i.e., the bar's longitudinal motion can be compared to that of the container.

The paper is divided as follows. In Section III, we model the system under two scenarios: one where the manipulator is left free of any actuation, and another where it is locked. In Section IV, the controller running on each vehicle is described, and, in Section VI, we linearize the system around the desired equilibrium and we study its stability. In Section VIII, we add an integral term to the controller, so as to compensate for model uncertainties; and in Section IX, we discuss the UAVs' attitude control. Finally, Section X provides an overview of the experimental setup and of the performed experiments.

This document is to be **read in conjunction with the mathematica notebook files** available in the repository.

The authors are with the School of Electrical Engineering, KTH Royal Institute of Technology, SE-100 44, Stockholm, Sweden. {ppereira, dimos}@kth.se. This work was supported by funding from the European Union's Horizon 2020 Research and Innovation Programme under the Grant Agreement No.644128 (AEROWORKS).

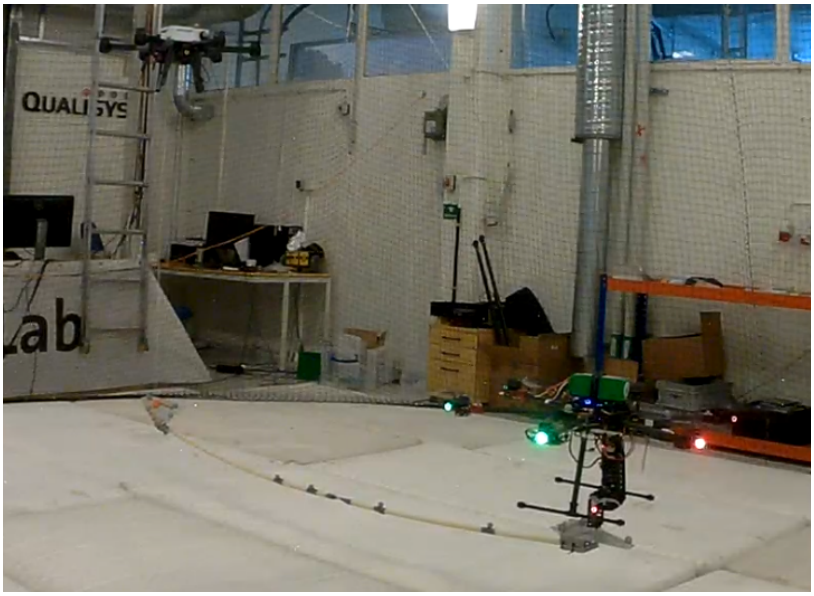

Fig. 1: Transportation of a bar object, grasped by a manipulator attached to one UAV, and connected to another UAV by means of a cable. The two UAVs are not identical, and two experiments were performed: one with the manipulator free of actuation, and another with the manipulator locked.

II. Notation

We denote $A_1 \oplus \cdots \oplus A_n$ as the block diagonal matrix with block diagonal entries A_1 to A_n (square matrices). $\mathbb{S}^1 := \{x \in \mathbb{R}^2 : x^T x = 1\}$ denotes the set of unit vectors in $\mathbb{R}^2$. We denote by $e_1, \cdots, e_n \in \mathbb{R}^n$ the canonical basis vectors in $\mathbb{R}^n$; when clear from the context, n is omitted. Given some $n, m \in \mathbb{N}$, and a function $f : \mathbb{R}^n \ni a \mapsto f(a) \in \mathbb{R}^m$, $Df : \mathbb{R}^n \ni a \mapsto Df(a) \in \mathbb{R}^{m \times n}$ denotes the derivative of f. Given two matrices A and B, $A \simeq B :\Leftrightarrow A = PBP^{-1}$ for some invertible matrix P.

III. Problem Description

Consider the system illustrated in Fig. 2, with two VTOL aerial vehicles (in our experimental case, two hexacopters); a one-dimensional-like bar; a rigid manipulator attached to one UAV, and with its end-effector attached to one contact point of the bar; and a cables connecting the other UAV to a distinct contact point of the bar. Hereafter, and for brevity, we refer to this bar+manipulator+tether+UAVs system as simply *the system*. Our modeling of the system is performed in two dimensions, and we leave for future work the inclusion and analysis of the lateral motion of the system. Moreover, in this first part, we consider the bar and the manipulator as rigid bodies, and the UAVs as point-masses; (later, in Section IX, we explain how to extend our analysis, when also considering the UAVs' attitude). We will be considering two systems, namely

1) the system with the manipulator free of actuation; and
2) the system with the manipulator locked (i.e., with a rigid grasping point).

We denote by $p_1, p_2, p_b, p_m \in \mathbb{R}^2$ the UAVs', the bar's and the manipulator's center of mass (CoM) positions; by $n_b, n_m \in \mathbb{S}^1$ the bar's and the manipulator's angular position; by $m_1, m_2, m_b, m_m > 0$ the UAVs', the bar's and the manipulator's masses; by J_b, J_m the bar's and the manipulator's moment of inertia; by l_1 the cables length; by l_m the distance between the CoM of the manipulator and its end-effector, and by l_2 the distance between the CoM of the UAV (to which the manipulator is attached) and the manipulator's end-effector. and, finally, by $d_1, d_2 \in \mathbb{R}$ the distance between the bar's CoM and the contact points on the bar to the cable and manipulator, respectively. Finally, we denote by $u_1, u_2 \in \mathbb{R}^3$ the UAVs' input forces, which we assume are inputs to the quadrotors-load system.

The system is then described by a position vector

$$P \in \mathbb{R}^{12} :\Leftrightarrow \begin{bmatrix} p_b \\ n_b \\ p_m \\ n_m \\ p_1 \\ p_2 \end{bmatrix} = \begin{bmatrix} \text{linear position of bar} \\ \text{angular position of bar} \\ \text{linear position of manipulator} \\ \text{angular position of manipulator} \\ \text{linear position of UAV 1} \\ \text{linear position of UAV 2} \end{bmatrix} \tag{1}$$

The system is composed of four linear positions (the bar's, the manipulator's, and the UAVs'), and therefore the potential

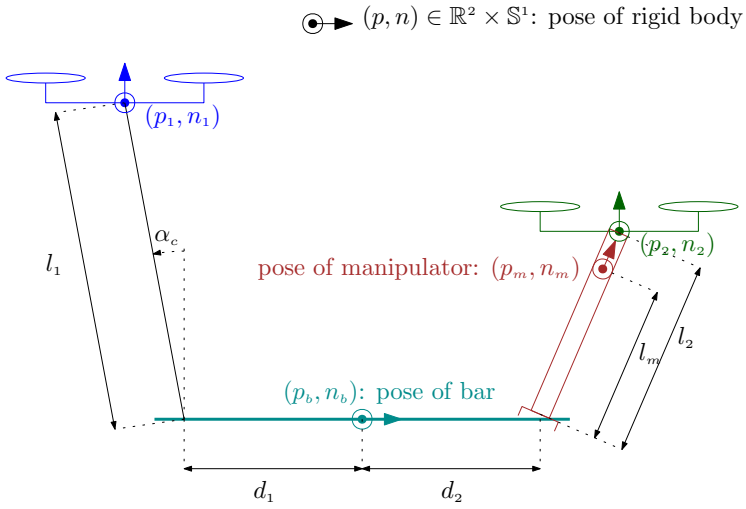

physical constants:
(m_b, J_b): mass and moment of inertia of bar
(m_m, J_m): mass and moment of inertia of manipulator
m_1, m_2: masses of UAVs

unit vectors expressed in terms of angles:
$n_b = (\cos(\alpha_b), \sin(\alpha_b))$
$n_m = (\ \sin(\alpha_m), \cos(\alpha_m))$
$\frac{p_1 - (p_b + d_1 n_b)}{l_1} = (\ \sin(\alpha_c), \cos(\alpha_c))$

Fig. 2: System composed of a rod-like object, a manipulator and two UAVs.

energy of the system with a position $P \in \mathbb{R}^{12}$ (as in (1)) is given by (below g stands for the acceleration due to gravity)

$$E_{\text{Potential}}(P) := \sum_{j \in \{b,m,1,2\}} g e_2^T p_j. \tag{2}$$

Additionally, the system is also composed of two angular positions (the bar's, the manipulator's), and therefore the kinetic energy of the system with velocity $\dot{P} \in \mathbb{R}^{12}$ is given by

$$E_{\text{Kinetic}}(\dot{P}) := \sum_{j \in \{b,m,1,2\}} m_j \frac{\|\dot{p}_j\|^2}{2} + \sum_{k \in \{b,m\}} J_j \frac{\|\dot{n}_j\|^2}{2}. \tag{3}$$

As explained, we consider two systems, and in both cases the system with position $P \in \mathbb{R}^{12}$ is constrained by several holonomic constraints. For the system when the manipulator is free there are seven holonomic constraints, namely

$$f^1(P) = 0_7 :\Leftrightarrow \begin{bmatrix} \|p_b + d_1 n_b - p_1\| - l_1 \\ p_b + d_2 n_b - p_2 - l_2 n_m \\ p_b + d_2 n_b - p_m - l_m n_m \\ n_b^T n_b - 1 \\ n_m^T n_m - 1 \end{bmatrix} = \begin{bmatrix} 0 \\ 0_2 \\ 0_2 \\ 0 \\ 0 \end{bmatrix}. \tag{4a}$$

while for the system where the manipulator is locked there are eight holonomic constraints, namely

$$f^2(P) = 0_8 :\Leftrightarrow \begin{bmatrix} f^1(P) \\ n_b^T n_m \end{bmatrix} = \begin{bmatrix} 0_7 \\ 0 \end{bmatrix}. \tag{4b}$$

The first three constraints in (4a) are geometric constraints that one can visualize in Fig. 2 (f.e, that the cable has length l_1). The last two constraints in (4a) simply constraint n_b and n_m to be unit vectors. The additional constraint in (4b) states that, when the manipulator is locked, the bar and the manipulator are orthogonal to each other. Given the constraints above, the first system may be described by $5 (= 12 - 7)$ generalized coordinates, while the second system may be described by $4 (= 12 - 8)$ generalized coordinates. Consider then the generalized coordinate, one for each system, (this choice is not

unique)

$$q^1 \in \mathbb{R}^5 :\Leftrightarrow \begin{bmatrix} p_b \in \mathbb{R}^2 \\ \alpha_b \in \mathbb{R} \\ \alpha_m \in \mathbb{R} \\ \alpha_c \in \mathbb{R} \end{bmatrix}, q^2 \in \mathbb{R}^4 :\Leftrightarrow \begin{bmatrix} p_b \in \mathbb{R}^2 \\ \alpha_b \in \mathbb{R} \\ \alpha_c \in \mathbb{R} \end{bmatrix} \tag{5}$$

whose components can be visualized in Fig 2. Consider also the maps g^1 and g^2 that convert, respectively, a generalized coordinate $q^1 \in \mathbb{R}^5$ and $q^2 \in \mathbb{R}^4$, into a position vector satisfying the constraint above. These maps are given by

$$\begin{aligned} g^i(q^i) &:= \begin{bmatrix} p_b \\ n_b \\ p_b + d_2 n_b + l_m n_m^i \\ n_m \\ p_b + d_1 n_b + l_1 n_c \\ p_b + d_2 n_b + l_2 n_m^i \end{bmatrix} \Big|_{\substack{n_b=(\cos(\alpha_b),\sin(\alpha_b)) \\ n_c=(-\sin(\alpha_c),\cos(\alpha_c))}} \in \mathbb{R}^{12}, \\ n_m^1 &= (-\sin(\alpha_m), \cos(\alpha_m)), \\ n_m^2 &= (-\sin(\alpha_b), \cos(\alpha_b)), \end{aligned}$$

where it is easy to verify that, indeed, $f^1(g^1(q^1)) = 0_7$ for all $q^1 \in \mathbb{R}^5$ and $f^2(g^2(q^2)) = 0_8$ for all $q^2 \in \mathbb{R}^4$, i.e., that g^1 and g^2 yield a position vector satisfying the holonomic constraints in (4a) and (4b), respectively.

We assume the UAVs are fully actuated, and thus we consider that we have available as inputs a two dimensional force on each UAV, namely

$$u \in \mathbb{R}^4 :\Leftrightarrow \begin{bmatrix} u_1 \in \mathbb{R}^2 \\ u_2 \in \mathbb{R}^2 \end{bmatrix} = \begin{bmatrix} \text{UAV's 1 input} \\ \text{UAV's 2 input} \end{bmatrix}.$$

Without hindering comprehension, hereafter, we omit the superscript 1 or 2 referring to whether we are considering the system with the manipulator free or locked. We only introduce $dq \equiv \dim(q)$ as the dimension of the generalized coordinate, and, as such, dq is 5 when the manipulator is free and 4 when it is locked. Let us denote as the state, the pair composed of the generalized position q and the generalized velocity $v = \dot{q}$, i.e.

$$x = (q, v) \equiv (q, \dot{q}) \in \mathbb{R}^{2dq}. \tag{6}$$

Given an appropriate input $u : \mathbb{R}_{\geq 0} \ni t \mapsto u(t) \in \mathbb{R}^4$, a trajectory $x : \mathbb{R}_{\geq 0} \ni t \mapsto x(t) \in \mathbb{R}^{2dq}$ evolves according to

$$\dot{x}(t) = X(x(t), u(t)), x(0) \in \mathbb{R}^{2dq},$$

where the (open-loop) vector field X is given by

$$X(x,u) := \begin{bmatrix} v \\ M^{-1}(q)\left(-C(q,v)v - G(q) + Dg(q)\begin{bmatrix} 0_8 \\ u \end{bmatrix}\right) \end{bmatrix} = \begin{bmatrix} \dot{q} \\ \dot{v} \end{bmatrix}, \tag{7}$$

with the matrices functions M, C and G found by means of the Lagrangian equations, which are themselves computed from the potential and kinetic energy functions in (2) and (3) We note that the vector field X above is only defined in a neighborhood of the origin (0_{2dq}), since the inverse $M^{-1}(q)$ is not defined for all $q \in \mathbb{R}^{dq}$. Nonetheless, we are interested in stability of the equilibrium

$$x^\star = 0_{2dq} :\Leftrightarrow (q^\star, v^\star) := (0_{dq}, 0_{dq}), \tag{8}$$

and it holds that $|M(0_{dq})| > 0$. As such the inverse exists around a neighborhood of the origin, which suffices for our purposes.

In order for (8) to qualify as an equilibrium, it must hold that $X(x^\star, u^\star) = 0_{2dq}$ for some equilibrium input $u^\star \in \mathbb{R}^4$. It follows that $u^\star$ is unique, and it is given by

$$\begin{aligned} &G(0_{dq}) = Dg(0_{dq}) \begin{bmatrix} 0_8 \\ u^\star \end{bmatrix} \Leftrightarrow u^\star := (u_1^\star, u_2^\star), \text{ where} \\ &u_1^\star := \left(m_1 g + \frac{d_2}{d_2 - d_1} m\right) e_2, \\ &u_2^\star := \left((m_2 + m_m) g + \frac{d_1}{d_1 - d_2} mg\right) e_2. \end{aligned}$$

That is, the UAV 1 must cancel its own weight, plus some of the weight of the bar; while UAV 2, in addition to its own weight, must also cancel the manipulator's weight, plus the remaing weight of the bar not canceled by UAV 1. The ratio of

$$|M^1(0_5)| = l_1^2 M_1 \left((m_b m_1 l_2^2 + m_m((l_2 - l_m)^2 m_2 + l_m^2 m_b) + J_m(m + m_2 + m_m)\left((d_1 - d_2)^2 m_1(m_2 + m_m) + (d_2^2(m_2 + m_m) + d_1^2 m_1)m_b + J_b(m_b + m_1 + m_2 + m_m)\right)\right)$$

$$|M^2(0_4)| = l_1^2 M_1 \left((m_b + m_2 + m_m)(m_1(m_2 + m_m)(d_1 - d_2)^2 + m_b(d_2^2(m_2 + m_m) + d_1^2 m_1)) + (m_b + m_1 + m_2 + m_m)((m_m + m_2 + m_m)(J_b + J_m) + l_2^2 m_b m_2 + (l_m^2 m_b + (l_2 - l_m)^2 m_2)m_m)\right)$$

the bar's weight distributed on each UAV is given by $\frac{d_2}{d_1}$, where the vehicle that carries more weight is that whose distance to the bar's center of mass is smaller: this agrees with intuition, which suggests that if one of the vehicles were connected to the bar's center-of-mass, then that vehicle would have to carry the whole weight of the bar (the other would only be used to control the attitude of the bar).

Problem 1: Given the vector field X in (7) and the equilibrium $x^\star$ in (8), design a control law $u^{cl} : \mathbb{R}^{12} \times \mathbb{R}^{12} \ni (P, \dot{P}) \mapsto u^{cl}(P, \dot{P}) \in \mathbb{R}^4$ satisfying $u^{cl}(g(q^\star), 0_{12}) = u^\star$ and such that $x^\star$ is an exponentially stable equilibrium of $\mathbb{R}^{2dq} \ni x \mapsto X(x, u^{cl}(g(q), Dg(q)v)) \in \mathbb{R}^{2dq}$.

Remark 1: In general, we may require the bar to stabilize around any point $p_b^\star \in \mathbb{R}^2$. For that purpose, it suffices only that the reference frame is chosen such that its origin coincides with $p_b^\star$, in which case we wish to stabilize around the equilibrium (8).

IV. Control law and closed loop

We consider each UAV is equipped with a PD controller, where given a system position $P \in \mathbb{R}^{12}$ and velocity $\dot{P} \in \mathbb{R}^{12}$,

$$u_1^{pd}(P, \dot{P}) := u_1^\star + m_1 \begin{bmatrix} -k_{p,x}^1(e_1^T p_1 - d_1) - k_{d,x}^1(e_1^T \dot{p}_1) \\ -k_{p,z}^1(e_2^T p_1 - l_1) - k_{d,z}^1(e_2^T \dot{p}_1) \end{bmatrix}$$

$$u_2^{pd}(P, \dot{P}) := u_2^\star + (m_2 + m_m) \begin{bmatrix} -k_{p,x}^2(e_1^T p_2 - d_2) - k_{d,x}^2(e_1^T \dot{p}_2) \\ -k_{p,z}^2(e_2^T p_2 - l_2) - k_{d,z}^2(e_2^T \dot{p}_2) \end{bmatrix}$$

where $k_{p,\star}^\star$ and $k_{d,\star}^\star$ are the proportional and derivative gains, along the x and z direction, and for UAVs 1 and 2. In the real control laws, the proportional and derivative errors are saturated, but since these do not interfere with the analysis we perform next, we omit this saturations here. The latter, leads to the complete control law

$$u^{pd}(P, \dot{P}) := \begin{bmatrix} u_1^{pd}(P, \dot{P}) \\ u_2^{pd}(P, \dot{P}) \end{bmatrix}. \tag{9}$$

One can then write the close loop vector field X^{cl}, namely

$$X^{cl}(x) := X(x, u^{pd}(P, \dot{P}))|_{P=g(q), \dot{P}=Dg(q)v}$$

which can then be used to compute the closed-loop state matrix

$$A := DX^{cl}(0_{2dq}) \in \mathbb{R}^{dq \times dq}. \tag{10}$$

Given Problem 1, our objective is thus to determine whether A is Hurwitz, in which case the equilibrium $x^\star := 0_{2dq}$ is (locally) exponentially stable.

V. Routh's criterion

In Sections VI and VII, we verify that the closed loop state matrix in (10) is similar to a block triangular matrix, whose block diagonal entries are in controllable form. This section provides immediate tools for the analysis of the eigenvalues of those matrices in controllable form. Denote then, for any $n \in \mathbb{N}$,

$$C_n(a) := \begin{bmatrix} 0 & 1 & 0 & \cdots & 0 \\ 0 & 0 & 1 & \cdots & 0 \\ \vdots & \vdots & \vdots & \ddots & \vdots \\ 0 & 0 & 0 & \cdots & 1 \\ -a_0 & -a_1 & -a_2 & \cdots & -a_{n-1} \end{bmatrix} \in \mathbb{R}^{n \times n},$$

which yields a matrix in controllable form, and whose eigenvalues are those in $\{\lambda \in \mathbb{C} : \sum_{i=0}^{i=n} a_i \lambda^i = 0\}$. It follows from the Routh's criterion that

$$C_2((a_0, a_1)) \text{is Hurwitz} \Leftrightarrow a_0, a_1 > 0, \tag{11}$$

$$C_3((a_0, a_1, a_2)) \text{is Hurwitz} \Leftrightarrow a_0, a_1, a_2 > 0 \wedge a_0 < a_1 a_2, \tag{12}$$

which we make use of later on. In what follows, let $f > 0$, $p \in \mathbb{R}$ and $k := (k_p, k_d) \in (\mathbb{R}_{\geq 0})^2$, where, in later sections, f and p provide physical constants of interest, and k provides the controller gains (in particular a proportional and a derivative gain). There is one matrix (in controllable form) that appears several times in Sections VI and VII, namely

$$\Gamma_4(f, p, k) := C_4(\nu)|_{\nu = (fk_p, fk_d, k_p + f(1+p), k_d)}. \tag{13}$$

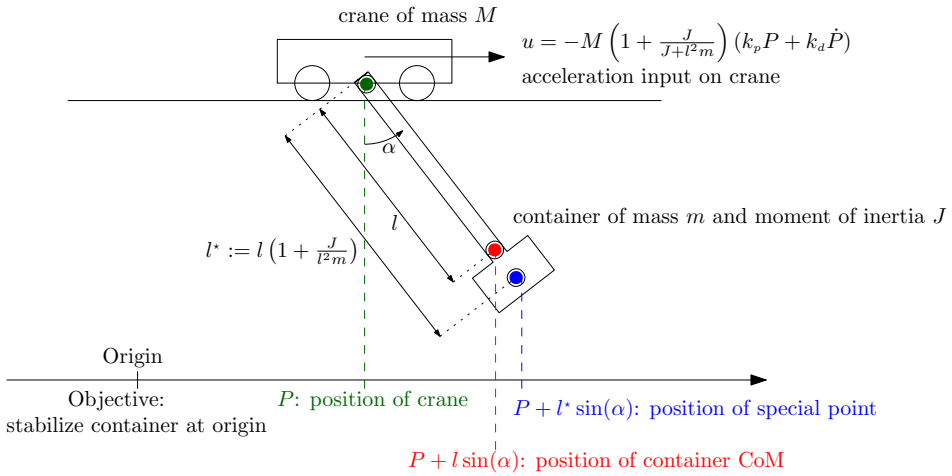

Fig. 3: Container-crane system: system composed of two UAVs, one manipulator and a bar may be compared to a container crane.

It follows from the Routh's criterion that (13) is Hurwitz, if and only if

$$p > 0. \tag{14}$$

A. Crane system

Let us give some intuition for the results that follow by considering a container-crane system, as illustrated in Fig. 3, where the goal is to stabilize the position of the container at the origin. If one writes the dynamics for this system (by means of its Lagrangian), under the control law shown in Fig. 3, one obtains a closed loop state matrix $A \in \mathbb{R}^{4\times 4}$, which is not in a form that allows for easy check of its eigenvalues (their location w.r.t. to the imaginary axis, to be more precise). This motivates the introduction of a similarity transformation, namely (next, $e_1, \cdots, e_4$ are the canonical basis vectors in $\mathbb{R}^4$)

$$P := \begin{bmatrix} p & Ap & A^2p & A^3p \end{bmatrix} \in \mathbb{R}^{4\times 4}, \tag{15}$$

$$p := e_1 + l^\star e_2 := e_1 + \frac{J + l^2 m}{lm} e_2 \in \mathbb{R}^4. \tag{16}$$

The position p in (16) is special (blue position in Fig. 3), because $A^3 p := -g e_4$, i.e., the jerk of the special point does not depend on any gains (this is not the case, if you consider other positions). If $A^3 p$ depended on gains, then $A^4 p$ would (likely) depend on products of gains, which complicates the stability analysis.

Recall now (13). It then follows that

$$\bar{A} := PAP^{-1} = \Gamma_4\left((f, p), (k_p, k_v)\right)$$

where

$$f = \frac{g}{l}\frac{l^2 m}{J + l^2 m}, \text{ and } p = \frac{l^2 m^2}{l^2 m M + J(m + M)} > 0.$$

Notice that f is the (squared) frequency of the pendulum (for a simple pendulum, where $J = 0$, $f = \frac{g}{l}$), and p is a positive adimensional parameter. If follows from (14) that PAP^{-1}, and therefore A, is Hurwitz; and therefore that, under the control law shown in Fig 3, the container is stabilized around the origin. One can also provide an interpretation for the similarity matrix P in (15): it implies that, for the linearized motion, the special position p defined in (16) behaves as a fourth order integrator, i.e.,

$$p^{(4)}(t) = \bar{A}_{4,1} p^{(0)}(t) + \cdots + \bar{A}_{4,4} p^{(3)}(t).$$

Studying the stability of this motion is equivalent to studying the location of the roots of the characteristic polynomial, i.e., $\{s \in \mathbb{C} : s^4 = \bar{A}_{4,1} s^0 + \cdots + \bar{A}_{4,4} s^3\}$, which justifies the results presented in Section V.

In what follows we will see that our system composed of two UAVs, one manipulator and a bar may be compared to a container crane. More specifically, the motion of a special point of the system has a similar behavior to that of the special point of the container.

VI. Free manipulator

As is, the state matrix A in (10) is unstructured (i.e., it is not a block diagonal matrix, nor block triangular, for example), and studying whether it is Hurwitz is not straightforward. Similarly to the crane system, this motivates the introduction of

a similarity matrix $P \in \mathbb{R}^{10\times 10}$, which will highlight the structure of the state matrix. We motivate the definition of the similarity matrix throughout this section. (In this section, e_i stands for the ith canonical basis vectors of $\mathbb{R}^n$, where n is clear from the context).

Similarly to the container-crane system, we introduce a special point, namely

$$p = e_1 + l^\star e_4\big|_{l^\star = \frac{J_m - l_m(l_2-l_m)m_m}{l_m m_b + (l_2-l_m)(m_m+m_m)}} \in \mathbb{R}^{10}, \tag{17}$$

for which $A^3 p$ (i.e., the jerk of the special point) also does not depend on any gains. Consider then

$$P := \begin{bmatrix} P_z & P_{\alpha_b} & P_p & P_\delta \end{bmatrix}^T \in \mathbb{R}^{10\times 10}, \tag{18}$$

where

$$\begin{aligned}
P_z &:= \begin{bmatrix} e_2 & Ae_2 \end{bmatrix} \in \mathbb{R}^{10\times 2},\\
P_{\alpha_b} &:= \begin{bmatrix} e_3 & Ae_3 \end{bmatrix} \in \mathbb{R}^{10\times 2},\\
P_p &:= \begin{bmatrix} p & Ap & A^2p & A^3p \end{bmatrix} \in \mathbb{R}^{10\times 4}, \text{ with } p \text{ as in (17)},\\
P_\delta &:= \begin{bmatrix} \nu & A\nu \end{bmatrix}|_{\nu = l_2 e_4 - l_1 e_5} \in \mathbb{R}^{10\times 2}.
\end{aligned}$$

Remark 2: Recall the generalized position q^1 in (5), and that, for the linearized motion, $\dot{x} = Ax$ with $x = (q^1, \dot{q}^1)$. Then note that (for brevity, denote $p_b =: (x, z)$),

$$\begin{aligned}
P_z^T(q^1, \dot{q}^1) &= (z^{(0)}, z^{(1)}),\\
P_{\alpha_b}^T(q^1, \dot{q}^1) &= (\alpha_b^{(0)}, \dot{\alpha}_b^{(1)}),\\
P_p^T(q^1, \dot{q}^1) &= (p^{\star(0)}, p^{\star(1)}, p^{\star(2)}, p^{\star(3)})|_{p^\star = x + l^\star \alpha_m},\\
P_\delta^T(q^1, \dot{q}^1) &= (l_2\alpha_m^{(0)} - l_1\alpha_c^{(0)}, l_2\alpha_m^{(1)} - l_1\alpha_c^{(1)}),
\end{aligned}$$

i.e., P_z is related with the z motion of the bar (2nd order system); P_{α_b} is related with the angular motion of the bar (2nd order system); P_p is related with the motion of the special point (4th order system), and, finally, P_δ is related with the angle-difference motion between the cable's and the manipulator's angles (2nd order system).

Let us introduce, for convenience, the following notation,

$$\star_i = \begin{bmatrix} f^1(k^1_{p,i}, k^2_{p,i}) \\ f^2(k^1_{d,i}, k^2_{d,i}) \end{bmatrix} \in \mathbb{R}^2, \text{ for } i \in \{x, z\},$$

where f^1 and f^2 are some affine functions (from $\mathbb{R}^2$ to $\mathbb{R}$); i.e., the first component of $\star_i$ is a function of the proportional gains of both vehicles, and the second component is a function of the derivative gains (either along the x direction, or the z direction).

Remark 3: For clarity of the presentation, in the results that follow we always make the assumption that $d_1 = -d_2 = d$ and that $l_m = l_2$; and we also denote $\bar{m}_2 := m_2 + m_m$. The results without these assumptions are found in mathematica notebook files.

Given the state matrix A in (10) and the similarly matrix P in (18), it then follows that

$$PAP^{-1} = A_{z,\alpha_b} \oplus A_{p,\delta} \in \mathbb{R}^{10\times 10}, \text{ where}$$

$$A_{z,\alpha_b} = \begin{bmatrix} A_z & e_2\bar{\star}_z^T \\ e_2\tilde{\star}_z^T & A_{\alpha_b} \end{bmatrix} \in \mathbb{R}^{(2+2)\times(2+2)}, \text{ and} \tag{19}$$

$$A_{p,\delta} = \begin{bmatrix} A_p & e_4\star_x^T \\ \star & A_\delta \end{bmatrix} \in \mathbb{R}^{(4+2)\times(4+2)}. \tag{20}$$

In order to simplify the analysis one can then choose the gains such that the matrices in (19) and (20) become block triangular. Regarding (19), one may choose to cancel either $\bar{\star}_z$ or $\tilde{\star}_z$. We opt for canceling $\bar{\star}_z$ (this will imply that the z linear motion of the bar is decoupled from the angular motion of the bar), which is satisfied if

$$\frac{k^1_{p,z}}{k^2_{p,z}} = \frac{k^1_{d,z}}{k^2_{d,z}} = \frac{(J_b + 2d^2 m_1)\bar{m}_2}{(J_b + 2d^2\bar{m}_2)m_1}.$$

That is, if the gains along the z direction of the vehicles satisfy the ratio above, then

$$A_{z,\alpha_b} = \begin{bmatrix} A_z & 0_{2\times 2} \\ \star & A_{\alpha_b} \end{bmatrix} \in \mathbb{R}^{(2+2)\times(2+2)}, \text{ where} \tag{21}$$

$$A_z = C_2(\gamma_z(k^2_{p,z}, k^2_{d,z})), A_{\alpha_b} = C_2(\gamma_{\alpha_b}(k^2_{p,z}, k^2_{d,z})), \tag{22}$$

and

$$\gamma_z = \frac{2(J_b + 2d^2 m_1)\bar{m}_2}{J_b(m_b + m_1 + \bar{m}_2) + d^2(4m_1\bar{m}_2 + m_b(m_1 + \bar{m}_2))}, \tag{23}$$

$$\gamma_{\alpha_b} = \frac{2d^2\bar{m}_2}{J_b + 2d^2\bar{m}_2}. \tag{24}$$

As such, it follows from (11), that A_z and A_θ (and therefore A_{z,α_b} in (21)) are Hurwitz.

Remark 4: Recall Remark 2, and denote $Z = (z^{(0)}, z^{(1)})$ and that $A = (\alpha_b^{(0)}, \alpha_b^{(1)})$. As such, it follows that for the linearized motion,

$$\begin{bmatrix} \dot{Z} \\ \dot{A} \end{bmatrix} = \begin{bmatrix} A_z & 0_{2\times 2} \\ \star & A_{\alpha_b} \end{bmatrix} \begin{bmatrix} Z \\ A \end{bmatrix},$$

that is, the z motion of the bar behaves as a second order integrator (see A_z in (22)) decoupled from the angular motion of the bar; while the angular motion of the bar also behaves as a second order integrator (see A_{α_b} in (22)), but coupled to the z motion of the bar.

Now, let us focus on (20). One possible option is to cancel $\star_x$, which is satisfied if $k^1_{p,x} = rk^2_{p,z} + \gamma$ and $k^1_{d,x} = rk^2_{d,z}$, for some $r, \gamma \in \mathbb{R}$. We follow a slightly different approach, and we do not cancel $\star_x$ entirely. First note that, when the manipulator is free of actuation, the system (see Fig. 2) is symmetric if $d_1 = d_2$, $l_1 = l_2 = l_m$, $m_1 = \bar{m}_2$, and $J_m = 0$. If we choose the gains along the x direction according to

$$\frac{k^1_{p,x}}{k^2_{p,z}} = \frac{k^1_{d,x}}{k^2_{d,z}} = \left(1 + \frac{J_m m_b}{(J_m + l_2^2 m_b)\bar{m}_2}\right).$$

then

$$A_{p,\delta} = \begin{bmatrix} A_p & \bar{\star} e_4 e_2^T \\ \tilde{\star} e_2 e_3^T & A_\delta \end{bmatrix} \in \mathbb{R}^{(4+2)\times(4+2)}, \tag{25}$$

where $\bar{\star}$ and $\tilde{\star}$ are the same (up to a multiplicative factor); they only depend on the physical constants (not on the gains); and they vanish when the symmetry conditions stated above are met. Moreover,

$$A_\delta = C_2((k^1_{p,x} + r, k^1_{d,x})), r > 0$$

which is Hurwitz (see (11)); and

$$A_p = \Gamma_4((f, p), (k^1_{p,x}, k^1_{d,x})),$$
$$f = \frac{g l_2(l_2(m_b + 2m_1) + l_1(m_b + 2\bar{m}_2)}{2l_1(J_m + l_2^2 m_b)}$$

and for some (adimensional) p that depends solely on the physical parameters – i.e., not on the gains (p is omitted for brevity). It follows from (14) that p provides a way of checking the stability (we believe it is positive for all physical parameters, but we cannot justify that statement at this point). Note however that (25) is not block triangular, but that $\bar{\star}$ and $\tilde{\star}$ vanish under symmetry conditions. As such, if the eigenvalues of A_δ and A_p are placed *far away* from the imaginary axis, and if the asymmetry of the system is *small enough*, then the eigenvalues of $A_{p,\delta}$ must also lie on the left of the imaginary axis (by continuity of the eigenvalues). Recal also the container-crane system described in Section V-A: it follows then that the special point p in (17) behaves as the special point of the container crane.

VII. Locked manipulator

Let us now focus on the system where the manipulator is locked, i.e., when the grasp is rigid. Similarly to as in Section VI, we need to find a similarity matrix $P \in \mathbb{R}^{8\times 8}$ (as opposed to $\mathbb{R}^{10\times 10}$), which will highlight the structure of the state matrix. We will motivate the definition of the similarity matrix throughout this section. Once again, e_i stands for the ith canonical basis vectors in $\mathbb{R}^n$, where n is assumed clear from the context.

Similarly to the container-crane system, we introduce a special point, namely

$$p = e_1 + l^\star e_4 \in \mathbb{R}^{10}, \tag{26}$$
$$l^\star = \frac{l_2 m_2 + l_m m_m}{m_b + m_2 + m_m}$$

for which $A^3 p$ also does not depend on any gains (i.e., the jerk of the special point does not depend on any gains). Consider then

$$P := \begin{bmatrix} P_z & P_{\alpha_b} & P_p \end{bmatrix}^T \in \mathbb{R}^{8\times 8}, \tag{27}$$

where

$$P_z := \begin{bmatrix} e_2 & Ae_2 \end{bmatrix} \in \mathbb{R}^{8\times 2},$$
$$P_{\alpha_b} := \begin{bmatrix} e_3 & Ae_3 \end{bmatrix} \in \mathbb{R}^{8\times 2},$$
$$P_p := \begin{bmatrix} p & Ap & A^2p & A^3p \end{bmatrix} \in \mathbb{R}^{8\times 4}, \text{ with } p \text{ as in (26)}$$

We point that an identical interpretation for the similarly matrix P can be drawn similarly to as in Remark 2. When the arm is locked we assume that the proportional and derivative gains of the vehicle carrying the arm are set to zero, i.e., that $k^2_{p,x} = 0$ and $k^2_{p,x} = 0$. The idea is that, when the arm is locked, it provides the necessary spring and damping action to stabilize the vehicle (carrying the manipulator) around its desired position. Notice that in Section VI, where the manipulator is free, the vertical linear and angular motion of the bar are decoupled from the rest of the other motions. When the arm is locked, this will no longer be the case.

Let us introduce, for convenience, the following notation,

$$\star_z = \begin{bmatrix} f^1(k^1_{p,z}, k^2_{p,z}) \\ f^2(k^1_{d,z}, k^2_{d,z}) \end{bmatrix} \in \mathbb{R}^2,$$
$$\star_{xz} = \begin{bmatrix} f^1(k^1_{p,x}, k^1_{p,z}, k^2_{p,z}) \\ f^2(k^1_{d,x}, k^1_{d,z}, k^2_{d,z}) \end{bmatrix} \in \mathbb{R}^2,$$

where f^1 and f^2 are some affine functions (from $\mathbb{R}^2$ to $\mathbb{R}$); i.e., the first component of $\star_\star$ is a function of the proportional gains of both vehicles, and the second component is a function of the derivative gains (either along the x direction, or the z direction).

Remark 5: For clarity of the presentation, in the results that follow we always make the assumption that $d_1 = -d_2 = d$, $l_m = l_2$. The results without these assumptions are found in the mathematica notebook files.

Given the similarity matrix P in (27) and the state matrix A in (10), it then follows that

$$PAP^{-1} = \begin{bmatrix} A_z & \gamma_1 e_2 \star_z^T & 0_{2\times 4} \\ \gamma_2 e_2 \star_z^T & A_{\alpha_b} & \gamma e_2 e_3^T \\ \gamma_3 e_2 \star_z^T & e_2 \star_{xz}^T & A_p \end{bmatrix}, \in \mathbb{R}^{(2+2+4)\times(2+2+4)} \tag{28}$$

where $\gamma, \gamma_1, \gamma_2, \gamma_3$ are constants (depending solely of the physical constants; not on the gains). The idea is, once again, to make the similar state matrix (i.e., PAP^{-1}) block triangular, and it is clear from (28) how to accomplish that. First, we choose the z gains such that the term $\star_z$ (showing trice in (28)) vanishes: that is accomplished if

$$\frac{k^1_{p,z}}{k^2_{p,z}} = \frac{k^1_{d,z}}{k^2_{d,z}} = \frac{m_2}{m_1}\frac{m_b + 2m_1}{m_b + 2\bar{m}_2},$$

i.e., if the gains along the z direction satisfy a specific ration. Then we choose the x gains such that the term $\star_{xz}$ (see (28)) vanishes: that is accomplished if

$$k^1_{p,x} = a + bk^2_{z,x}$$
$$k^1_{d,x} = bk^2_{d,x}$$

where a and b are constants found in the mathematica files. If the choices above are satisfied, it follows that

$$PAP^{-1} = \begin{bmatrix} A_z \oplus A_{\alpha_b} & \gamma e_4 e_3^T \\ 0_{4\times 4} & A_p \end{bmatrix}, \in \mathbb{R}^{(4+4)\times(4+4)}$$

for some $\gamma \in \mathbb{R}$, and where

$$A_z = C_2(\gamma_z(k^2_{p,z}, k^2_{d,z})), \gamma_z > 0,$$
$$A_{\alpha_b} = C_2(\gamma_{\alpha_b}(k^2_{p,z}, k^2_{d,z})), \gamma_{\alpha_b} > 0,$$

and where

$$A_p = \Gamma_4((f, p), (k^1_{p,x}, k^1_{d,x}))$$
$$f = \frac{g}{l_1}\frac{m_b + 2m_1}{2(m_b + \bar{m}_2)}, p > 0.$$

As such, it follows from (11) and (14) that A_z, A_{α_b} and A_p are Hurwitz, and therefore that the state matrix A is also Hurwitz.

VIII. Integral action

In this section, we augment the previous control in (9) with integral action terms, that provide robustness against model uncertainties, such as an unknown bar mass. For this purpose, we augment the state x in (6) as

$$\bar{x} = (x, \xi_1, \xi_2) \in \mathbb{R}^{10+2} \tag{29}$$

and we augment the vector field X in (7) as

$$\bar{X}(\bar{x}, u) = \begin{bmatrix} X(x,u) \\ e_2^T p_1 - l_1 \\ e_2^T p_2 - l_2 \end{bmatrix} = \begin{bmatrix} \dot{x} \\ \dot{\xi}_1 \\ \dot{\xi}_2 \end{bmatrix},$$

and, as such, one may interpret ξ_1, ξ_2 as the vertical integral errors for each vehicle. We then augment the previous control law u^{PD} in (9) , by using the integral terms, specifically

$$u^{pid}(\bar{x}) = \begin{bmatrix} u_1^{pd}(x) \\ u_2^{pd}(x) \end{bmatrix} - \begin{bmatrix} m_1 k_{i,z}^1 \xi_1 e_2 \\ (m_2 + m_m) k_{i,z}^2 \xi_2 e_2 \end{bmatrix},$$

where $k_{i,z}^1, k_{i,z}^2$ are the positive integral gains. One can then write the augmented close loop vector field $\bar{X}^{cl}(\bar{x}) := \bar{X}(\bar{x}, u^{pid}(\bar{x}))$, and from which one derives the augmented closed loop state matrix $\bar{A} := D\bar{X}^{cl}(0_{12}) \in \mathbb{R}^{12\times 12}$.

Consider then the augmented similarly matrix $\bar{P} \in \mathbb{R}^{12\times 12}$ similarly to (18), with the only difference that

$$\bar{P}_z := \begin{bmatrix} \nu & A\nu & A^2\nu \end{bmatrix}|_{\nu = \frac{1}{d_1 - d_2}(-d_2 e_{11} + d_1 e_{12})} \in \mathbb{R}^{12\times 3},$$
$$\bar{P}_{\alpha_b} := \begin{bmatrix} \nu & A\nu & A^2\nu \end{bmatrix}|_{\nu = \frac{1}{d_1 - d_2}(e_{11} - e_{12})} \in \mathbb{R}^{12\times 3}.$$

Remark 6: Recall the augmented state $\bar{x}$ in (29), and that, for the linearized motion, $\dot{\bar{x}} = \bar{A}\bar{x}$. Then note that (for brevity, denote $p_b =: (x, z)$)

$$(d_1 - d_2)\bar{P}_z^T \bar{x} = (z^{(-1)}, z^{(0)}, z^{(1)}) = (-d_2\dot{\xi}_1 + d_1\dot{\xi}_2, z, \dot{z}),$$
$$(d_1 - d_2)\bar{P}_{\alpha_b} \bar{x} = (\alpha_b^{(-1)}, \alpha_b^{(0)}, \alpha_b^{(1)}) = (\dot{\xi}_1 - \dot{\xi}_2, \alpha_b, \dot{\alpha}_b),$$

i.e., the sum of the integral errors (weighted by d_1 and d_2) is related to the z motion of the bar (3rd order system); and the difference between the integral errors is related to the angular motion of the bar (3rd order system).

Let us introduce, for convenience, the following notation,

$$\star_z = \begin{bmatrix} f^1(k_{i,z}^1, k_{i,z}^2) \\ f^2(k_{p,z}^1, k_{p,z}^2) \\ f^3(k_{d,z}^1, k_{d,z}^2) \end{bmatrix} \in \mathbb{R}^3,$$

where f^1, f^2, f^3 are affine functions (from $\mathbb{R}^2$ to $\mathbb{R}$). Given the augmented similarity matrix $\bar{P}$ and the augmented state matrix $\bar{A}$, it then follows that

$$\bar{P}\bar{A}\bar{P}^{-1} = \bar{A}_{z,\alpha_b} \oplus \bar{A}_{p,\delta} \in \mathbb{R}^{(6+6)\times(6+6)},$$

where $\bar{A}_{p,\delta} \in \mathbb{R}^{6\times 6}$ is exactly the same as in (20), while $\bar{A}_{z,\alpha_b}$ is different, namely

$$\bar{A}_{z,\alpha_b} = \begin{bmatrix} \bar{A}_z & e_3 \bar{\star}_z^T \\ e_3 \tilde{\star}_z^T & \bar{A}_{\alpha_b} \end{bmatrix} \in \mathbb{R}^{(3+3)\times(3+3)}. \tag{30}$$

In order to simplify the analysis one can then choose the gains such that the matrix in (30) becomes block triangular. One may choose to cancel either $\bar{\star}_z$ or $\tilde{\star}_z$. We opt for canceling $\bar{\star}_z$ (this will imply that the z linear motion of the bar is decoupled for the angular motion of the bar), which is satisfied if

$$\frac{k_{i,z}^1}{k_{i,z}^2} = \frac{k_{p,z}^1}{k_{p,z}^2} = \frac{k_{d,z}^1}{k_{d,z}^2} = \frac{(J_b + 2d^2 m_1)\bar{m}_2}{(J_b + 2d^2\bar{m}_2)m_1}.$$

That is, if the gains along the z direction of the vehicles satisfy the ratio above, then

$$\bar{A}_{z,\alpha_b} = \begin{bmatrix} \bar{A}_z & 0_{3\times 3} \\ e_3 \tilde{\star}_z^T & \bar{A}_{\alpha_b} \end{bmatrix} \in \mathbb{R}^{(3+3)\times(3+3)}$$
$$\bar{A}_z = C_3(\gamma_z(k_{i,z}^2, k_{p,z}^2, k_{d,z}^2)), \bar{A}_{\alpha_b} = C_2(\gamma_{\alpha_b}(k_{i,z}^2, k_{p,z}^2, k_{d,z}^2)),$$

with γ_z and γ_{α_b} as in (23) and (24). It then follows from (12) that $\bar{A}_{z,\alpha_b}$ is Hurwitz if

$$k_{i,z}^2 < \min(\gamma_z, \gamma_{\alpha_b}) k_{p,z}^2 k_{d,z}^2.$$

The constraint above is stricter than for a *normal* PID, where $k_{i,z}^2 < k_{p,z}^2 k_{d,z}^2$ applies. That is the case because $\gamma_{\alpha_b} < 1$ (see (24)), and notice that γ_{α_b} – which is associated with the z angular motion of the bar – vanishes when d vanishes. This agrees with intuition, which suggests that controlling the attitude of the bar is *difficult* when the contact points are too close to the bar's center of mass.

IX. Attitude inner loop

In the previous sections, we assume the vehicles were point masses and fully actuated. In practice, though, each vehicle has a thrust direction, along which a thrust input may be provided. This thrust direction is then controlled via an attitude inner loop, which tries to pull the thrust direction towards the desired thrust direction (which is the direction the vehicle would have, if it were fully actuated).

In order to analyze this system, one needs to extend the state x in (6) with the attitude position and attitude velocity of each vehicle, i.e.,

$$\tilde{x} = (x, \alpha_1, \alpha_2, \omega_1, \omega_2) \in \mathbb{R}^{2dq+4}$$

where $n_i = (\sin(\alpha_i), \cos(\alpha_i)) \in \mathbb{S}^1$ is the thrust direction of vehicle $i \in \{1, 2\}$; one must then also extend the vector field X in (7) as

$$\tilde{X}(\tilde{x}, u) = \begin{bmatrix} X(x, (u_1^T n_1 n_1, u_2^T n_2 n_2)) \\ \omega_1 \\ \omega_2 \\ J_1^{-1}\left(-k_{d,\alpha}^1 n_1^T \frac{u_1}{\|u_1\|} - k_{d,\alpha}^1 \omega_1\right) \\ J_2^{-1}\left(-k_{d,\alpha}^2 n_2^T \frac{u_2}{\|u_2\|} - k_{d,\alpha}^2 \omega_2\right) \end{bmatrix} = \begin{bmatrix} \dot{x} \\ \dot{\alpha}_1 \\ \dot{\alpha}_2 \\ \dot{\omega}_1 \\ \dot{\omega}_2 \end{bmatrix},$$

where $J_i, k_{p,\alpha}^i, k_{d,\alpha}^i$ are the inertia, the attitude proportional gain, and the attitude derivative gain of vehicle $i \in \{1, 2\}$. For the model above, if $n_i = \frac{u_i}{\|u_i\|}$ for $i \in \{1, 2\}$, then $(u_1^T n_1 n_1, u_2^T n_2 n_2) = (u_1, u_2)$. As such, for attitude gains sufficiently big, one excepts $X(x, (u_1^T n_1 n_1, u_2^T n_2 n_2)) \approx X(x, (u_1, u_2))$, in which case one may invoke the results from the previous sections. We leave for future work finding lower bounds on the attitude gains that guarantee exponential stability of the equilibrium.

X. Experiments

A complete video showing the whole experimental procedure is available at https://youtu.be/Cirzxkdloq0. We resort to an experimental setup composed of two different aerial vehicles - an Asctec Neo and a custom platform, denominated Popeye - and a Qualisys motion capture system that works at 100Hz. The Neo and the Popeye have masses, respectively, of 2.2 kg and 2.7 kg. The AscTec Neo is equipped with a cable that is 1.5 m long, while the Popeye is equipped with a two degree-of-freedom arm (as such, the arm can rotate independently of the bar or the vehicle, while keeping a rigid grasp on the end-effector). The arm has a mass of 0.9 kg, and the arm links are 0.32m and 0.1m long, respectively, for the first and the second links (the first one being the closest to the vehicle center of mass). The two joints are located between the vehicle frame and the first link, and between the first and second links, respectively. On our experiments, the joints were either not actuated (free of actuation) or they were locked (this was mocked by choosing high gains for the joints PIDs; in this case, the whole arm behaves like a rigid bar). The Neo has a permanent magnet at the end of the cable, while the Popeye has an electromagnet as an end-effector (the electromagnet is strong enough so that there is no significant slippage at the point of contact). The bar to be transported has mass of approximately of 1.5kg, with metal plates at its end points, which are the grasping points for the permanent magnet (Neo) and the electromagnet (Popeye).

In order to observe the convergence properties of our system, a trajectory composed of four types of sepoints was tested: motion along the world z-axis (pickup and drop-off), motion along the world x-axis, motion along the world y-axis, and a rotation around the world z-axis. These setpoints test if the system is able to accomplish object translations and rotations. The results are shown in Fig. 4.

Figures 4(a) and 4(b) show the position and attitude of the bar for the whole experiment. The Neo and Popeye positions and control inputs are shown in Figs. 4(c)- 4(d) and 4(e)-4(f), respectively. The experiment starts by moving the vehicles to the respective setpoints for pickup. Firstly, Popeye goes for the pickup pose and attaches itself to the bar (by means of the electromagnet). Secondly, Neo goes to the setpoint above its pickup location. At $t_1 = 90$s, the vehicles start the bar pick-up. At this point, the thrust inputs start increasing as the integrals start compensating for the static error (allowing for the bar to be picked-up) – see Figs. 4(g), 4(e) and 4(f). After both UAVs stabilize at around $t_2 = 120$s, two setpoints are consecutevily given to the bar as a motion towards the negative x-axis on the world frame – see Fig 4(a). After this translation, a rotation is applied to the bar at around $t_3 = 135$s, as seen in Fig 4(b). When the system stabilizes, two consecutive setpoints are applied along the $-y$ and $+y$-axis on the world frame at around $t_4 = 150$s – see Fig 4(a). Finally, to test if the system is robust to external disturbances, a non-modeled external force is applied on the Popeye three times, at around $t_5 = 175$s –

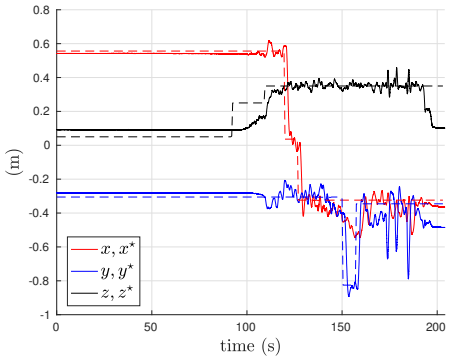

(a) Bar position

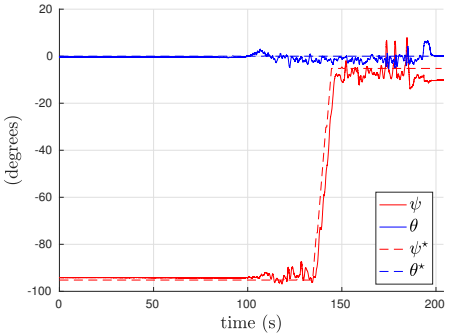

(b) Bar attitude

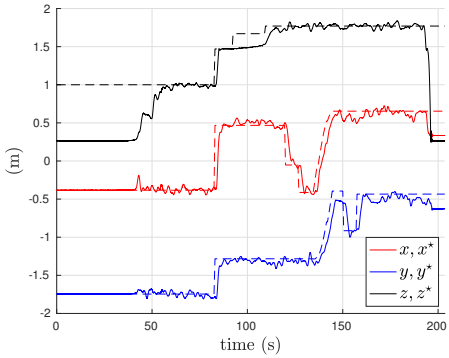

(c) ASTEC-Neo position

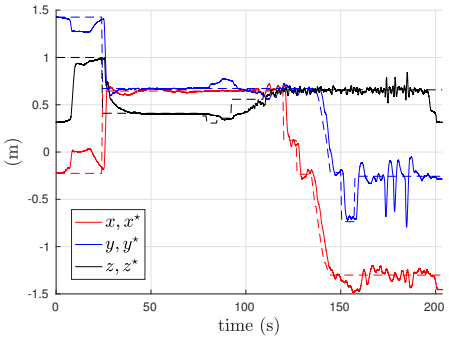

(d) Popeye position

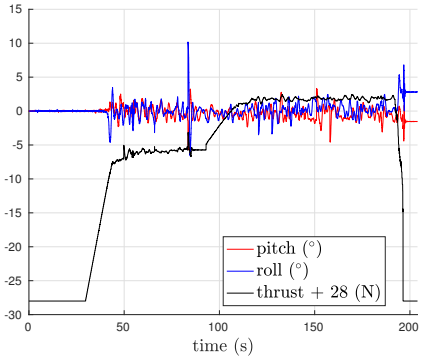

(e) ASTEC-Neo inputs (mav_msgs/RollPitchYawrateThrust)

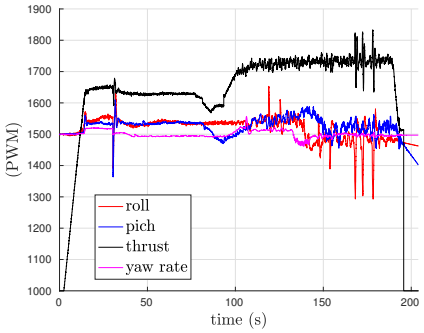

(f) Popeye inputs (mavros_msgs/OverrideRCIn)

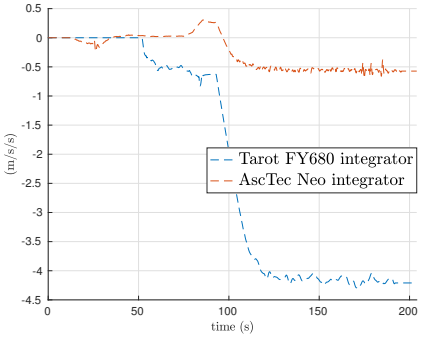

(g) UAV's integral terms

Fig. 4: Experimental results for pose stabilization of a bar tethered to one AscTec Neo and grasped by a manipulator coupled to a Tarot FY680.

see Fig 4(d); this disturbance has a pronounced effect on the bar's position, as can be seen in Fig 4(a). At around 190s, a landing command is given to both vehicles. As it is observed, position and attitude convergence is achieved for the motions performed through t_1 to t_4. Robustness to external disturbances is also achieved, as the system successfully stabilizes after being excited by an unmodeled force, as seen after t_5.

XI. Conclusion

In this manuscript a pose stabilization controller was proposed for an object being transported by two non-identical UAVs, one manipulator-endowed and the other tether-endowed. The experimental results show that the controller robustly stabilizes around different set-points and in the presence of external disturbances.

Future work will focus on enabling the UAVs to operate outdoors, in the absence of a motion capture system. In particular, we will focus on vision algorithms to detect the object grasping points based on feature extraction, on relative and absolute localization methods and on estimation algorithms that can enable safe navigation on different scenarios.

References

[1] M. Gassner, T. Cieslewski, and D. Scaramuzza. Dynamic collaboration without communication: Vision-based cable-suspended load transport with two quadrotors. In *2017 IEEE International Conference on Robotics and Automation (ICRA)*, pages 5196–5202, May 2017.

[2] S. Kim, S. Choi, H. Lee, and H. J. Kim. Vision-based collaborative lifting using quadrotor uavs. In *2014 14th International Conference on Control, Automation and Systems (ICCAS 2014)*, pages 1169–1174, Oct 2014.

[3] C. Masone, H. H. Bülthoff, and P. Stegagno. Cooperative transportation of a payload using quadrotors: A reconfigurable cable-driven parallel robot. In *2016 IEEE/RSJ International Conference on Intelligent Robots and Systems (IROS)*, pages 1623–1630, Oct 2016.

[4] A. Tagliabue, M. Kamel, S. Verling, R. Siegwart, and J. Nieto. Collaborative transportation using mavs via passive force control. In *2017 IEEE International Conference on Robotics and Automation (ICRA)*, pages 5766–5773, May 2017.

[5] P. Pereira and Dimos V. Dimarogonas. Collaborative transportation of a bar by two aerial vehicles with attitude inner loop and experimental validation. In *2017 Conference on Decision and Control*, 2017 (to appear).

[6] T. Lee. Collision avoidance for quadrotor uavs transporting a payload via voronoi tessellation. In *2015 American Control Conference (ACC)*, pages 1842–1848, July 2015.

[7] Q. Jiang and V. Kumar. The inverse kinematics of cooperative transport with multiple aerial robots. *IEEE Transactions on Robotics*, 29(1):136–145, Feb 2013.

[8] Hyeonbeom Lee, Hyoin Kim, and H. J. Kim. Path planning and control of multiple aerial manipulators for a cooperative transportation. In *2015 IEEE/RSJ International Conference on Intelligent Robots and Systems (IROS)*, pages 2386–2391, Sept 2015.

[9] S. J. Lee and H. J. Kim. Autonomous swing-angle estimation for stable slung-load flight of multi-rotor uavs. In *2017 IEEE International Conference on Robotics and Automation (ICRA)*, pages 4576–4581, May 2017.

[10] Daniel Mellinger, Michael Shomin, Nathan Michael, and Vijay Kumar. Cooperative grasping and transport using multiple quadrotors. In *Distributed autonomous robotic systems*, pages 545–558. Springer, 2013.

[11] G. Gioioso, A. Franchi, G. Salvietti, S. Scheggi, and D. Prattichizzo. The flying hand: A formation of uavs for cooperative aerial tele-manipulation. In *2014 IEEE International Conference on Robotics and Automation (ICRA)*, pages 4335–4341, May 2014.

[12] M. Mohammadi, A. Franchi, D. Barcelli, and D. Prattichizzo. Cooperative aerial tele-manipulation with haptic feedback. In *2016 IEEE/RSJ International Conference on Intelligent Robots and Systems (IROS)*, pages 5092–5098, Oct 2016.

[13] M. Bisgaard, A. la Cour-Harbo, and J. D. Bendtsen. Adaptive control system for autonomous helicopter slung load operations. *Control Engineering Practice*, 18(7):800 – 811, 2010. Special Issue on Aerial Robotics.

[14] Nathan Michael, Jonathan Fink, and Vijay Kumar. Cooperative manipulation and transportation with aerial robots. *Autonomous Robots*, 30(1):73–86, Jan 2011.

[15] D. Mellinger, Q. Lindsey, M. Shomin, and V. Kumar. Design, modeling, estimation and control for aerial grasping and manipulation. In *2011 IEEE/RSJ International Conference on Intelligent Robots and Systems*, pages 2668–2673, Sept 2011.

[16] P. E. I. Pounds, D. R. Bersak, and A. M. Dollar. Grasping from the air: Hovering capture and load stability. In *2011 IEEE International Conference on Robotics and Automation*, pages 2491–2498, May 2011.

[17] R. Mebarki, V. Lippiello, and B. Siciliano. Toward image-based visual servoing for cooperative aerial manipulation. In *2015 IEEE International Conference on Robotics and Automation (ICRA)*, pages 6074–6080, May 2015.

[18] R. Mebarki, V. Lippiello, and B. Siciliano. Image-based control for dynamically cross-coupled aerial manipulation. In *2014 IEEE/RSJ International Conference on Intelligent Robots and Systems*, pages 4827–4833, Sept 2014.

[19] V. Ghadiok, J. Goldin, and W. Ren. Autonomous indoor aerial gripping using a quadrotor. In *2011 IEEE/RSJ International Conference on Intelligent Robots and Systems*, pages 4645–4651, Sept 2011.

[20] A. Q. L. Keemink, M. Fumagalli, S. Stramigioli, and R. Carloni. Mechanical design of a manipulation system for unmanned aerial vehicles. In *2012 IEEE International Conference on Robotics and Automation*, pages 3147–3152, May 2012.

[21] A. Gawel, M. Kamel, T. Novkovic, J. Widauer, D. Schindler, B. P. von Altishofen, R. Siegwart, and J. Nieto. Aerial picking and delivery of magnetic objects with mavs. In *2017 IEEE International Conference on Robotics and Automation (ICRA)*, pages 5746–5752, May 2017.

[22] H. Lee, H. Kim, and H. J. Kim. Planning and control for collision-free cooperative aerial transportation. *IEEE Transactions on Automation Science and Engineering*, PP(99):1–13, 2017.

[23] N. Staub, M. Mohammadi, D. Bicego, D. Prattichizzo, and A. Franchi. Towards robotic magmas: Multiple aerial-ground manipulator systems. In *2017 IEEE International Conference on Robotics and Automation (ICRA)*, pages 1307–1312, May 2017.

[24] J. Schultz and T. Murphey. Trajectory generation for underactuated control of a suspended mass. In *2012 IEEE International Conference on Robotics and Automation*, pages 123–129, May 2012.

[25] P. O. Pereira and D. V. Dimarogonas. Stability of load lifting by a quadrotor under attitude control delay. In *2017 IEEE ICRA*, pages 3287–3292, May 2017.

[26] M. Orsag, C. Korpela, M. Pekala, and P. Oh. Stability control in aerial manipulation. In *2013 American Control Conference*, pages 5581–5586, June 2013.